

# Synergistic action of flavin containing NADH dependant azoreductase and cytochrome P450 monooxygenase in azoaromatic mineralization†

Cite this: *RSC Advances*, 2013, 3, 3062

Chetan C. Oturkar,<sup>a</sup> Munif A. Othman,<sup>b</sup> Mahesh Kulkarni,<sup>c</sup> Datta Madamwar<sup>c</sup> and Kachru R. Gawai<sup>\*b</sup>

An alkaliphilic strain *Bacillus lentus* BI377 was isolated from contaminated soil of the textile area of Solapur, India. The strain was able to degrade almost 98% of recalcitrant azoic compounds by a mutually regulated process of azoreductase and a monooxygenase system. An enzyme activity study and a periodical carbon monoxide (CO) binding spectra study on a UV-visible spectrophotometer revealed that the intermediate amines formed by typical azoreduction (N=N cleavage), subsequently underwent hydroxylation by the cytochrome P450 monooxygenase (CYP450) system. Azoreductase was purified by chromatographic techniques and characterization by MALDI-TOF substantiated its identity as FMN containing NADH dependent azoreductase of 32 kDa in size. Surprisingly, purified azoreductase showed the highest activity at 80 °C and pH 8.0. An increase in the activity of superoxide dismutase after decolorization confirmed the signature of oxidative stress and its involvement in the dismutation of reactive metabolites. Intermediate metabolite analysis by HPLC, GC-MS and FTIR and the removal of total organic carbon (TOC) suggested the azoaromatics' degradation leads to mineralization *via* a TCA cycle.

Received 18th April 2012,  
Accepted 16th December 2012

DOI: 10.1039/c2ra21389c

[www.rsc.org/advances](http://www.rsc.org/advances)

## Introduction

Azoic compounds constitute the largest group of mutagenic and carcinogenic xenobiotics that are commonly discharged into the ecosystem.<sup>1,2</sup> They are characterized by aromatic moieties, generally benzene or naphthalene groups, linked together with one or more azo groups (–N=N–), which may contain different substituents, such as chloro (–Cl), methyl (–CH<sub>3</sub>), nitro (–NO<sub>2</sub>), amino (–NH<sub>2</sub>), hydroxyl (–OH), carboxyl (–COOH) or sulfonic (–SO<sub>3</sub>H) groups.<sup>3</sup> Apart from the conventional approaches to dye removal,<sup>2</sup> the increasing demand for economically feasible enzyme associated bioprocesses seems to offer an enormous potential to provide whole cell biocatalysts with great applicability.<sup>2,4</sup> In the last two decades, there has been a tremendous upsurge in the exploitation of ecofriendly alternatives to deal with azoaromatics' bioremediation. The redox potential generated by an anaerobic–aerobic process accelerates site specific cleavage in complex aromatics so that electron withdrawing azo linkages, which are very resistant to oxidative reactions, can be reduced under

anaerobic conditions to yield aromatic amines which are in turn likely to be removed by aerobic treatment.<sup>1,2,5,6</sup> The typical reduction of these azoaromatic compounds is mainly attributed to azoreductase, which cleaves the azo bond by a ping pong mechanism, using NADH or NADPH as a cofactor.<sup>1,2,7</sup> The attainment of azo bond cleavage leads to another problem as it generates toxic amines or reactive oxygen species, which are intermediate metabolites in biomass.<sup>8</sup> This unexpected bioactive interference creates a burden on cells and hinders the degradation/mineralization process by affecting the growth of biomass or by enzyme repression.<sup>9</sup> To overcome this problematic intermediate saturation, a sequential anaerobic–aerobic bioreactor has been increasingly employed as an ecofriendly alternative.<sup>6,7</sup> In light of recent developments in bioremediation, aerobic–anaerobic processes will be difficult to justify because of their time consuming nature and high cost.

CYP450 is the main component of the mixed function oxidase system with great catalytic versatility and plays an important role in the biotransformation of a wide variety of xenobiotics.<sup>10</sup> A literature survey reveals that its induction in response to aromatic amines<sup>10–12</sup> continues as nucleophilic reactions so that the hydrophilicity of these reactive metabolites will be utilized as a source of energy *via* the central metabolic pathway (TCA cycle) in bacteria.<sup>12,13</sup> The current experimental practice of utilizing lacasse enzymes for the oxidative cleavage of azo dyes reflects the single step nature of

<sup>a</sup>BRD School of Biosciences, Sardar Patel University, Vallabh Vidyanagar, India.

E-mail: [chetanvc@gmail.com](mailto:chetanvc@gmail.com)

<sup>b</sup>Department of Chemistry, University of Pune, India.

E-mail: [chetanvc2000@yahoo.com](mailto:chetanvc2000@yahoo.com); Fax: +91-020-25691728; Tel: +91-020- 2569606

<sup>c</sup>Center for Material Characterization, National Chemical Laboratory, Pune, India

† Electronic supplementary information (ESI) available: Details of UV Visible spectra of dye decolorization, GC-MS fragmentation and FTIR frequencies, substrate specificity study, MALDI-TOF MSMS ion peaks of azoreductase.

the degradation, which results from its ability to use single molecular oxygen as an electron acceptor, despite the cofactor being present, non-specific oxidation,<sup>4</sup> highly non-specific free radical mechanism and the formation of phenolic type compounds.<sup>9</sup> Moreover, various oxidoreductase activities have been tested using consortia with the highest reductase and oxygenase activity *e.g.* from *Pseudomonas putida* MET 94 and *Bacillus subtilis* for ecofriendly degradation or mineralization respectively.<sup>5,14</sup> It has been observed that bacteria contain the flavin-diffusible monooxygenase (FDM) system in which free, reduced flavin is first generated by the flavin reductase component of the enzyme and then transferred to the oxygenase component for activation.<sup>15</sup> However, bacterial biotransforming enzymes have significant limitations due to physicochemical factors like temperature, concentration and the nature of xenobiotics.<sup>16</sup> Hence, it is a prerequisite to isolate a strain with superior redox machinery to facilitate microbial reactions even under extreme conditions. Recently, research on thermostable azoreductases has come into the limelight and focuses on the reduction of azoaromatics at high temperature *e.g.* azoreductase from *G. stearothermophilus* was found to be active at 60 °C.<sup>17</sup> Previously, we reported the isolation and identification of potential soil isolate *Bacillus lentus* BI377 (*B. lentus* BI377) and its considerable catabolic diversity towards sulphonated dyes.<sup>18</sup>

With this in mind, a mechanistic study of azoic mineralization was carried out using a wide range of azo dyes *viz.* Red120 (RR120), Red141 (RR141), Red2 (RR2), Red11 (RR11) Sunset Yellow (SY) and Tartrazine (TAR), and the intermediate moieties formed during biodegradation were analyzed by gas chromatography–mass spectroscopy (GC-MS), Fourier transform infrared (FTIR) and high-performance liquid chromatography (HPLC) to elucidate a plausible degradation pathway. Also, in the present study, it is the first time that a successful attempt has been made to purify and characterize azoreductase from the gram positive alkaliphilic *B. lentus* BI377. The critical role of the CYP450 monooxygenase system and superoxide dismutase (SOD) in the process of mineralization was also studied by a carbon monoxide (CO) binding assay and an enzyme activity study.

## Results and discussion

### Whole cell decolourization assessment

The decolourization percentage and the shift in the original absorbance of each dye were monitored every 2 h till the complete decolorization under static conditions was achieved (ESI Fig. S1†), and the relevant enzyme activity studies of the control as well as the decolorized sample were measured as shown in Table 1. Almost 75% decolorization was observed in the case of all azo dyes within 4 h, whereas, eight hours after the culture was supplemented with azoic dyes, 99% decolorization was established. Significant azoreductase activity was noted at 4 h, which was independent of NADH or NADPH<sup>1,2</sup> since the reduction reaction with the purified enzyme takes place in the presence of such cofactors. Maximum decolorization was achieved with a linear growth in biomass at optimum pH 8.0. Whereas, a gradual decrease in the original absorbance with an increasing activity of azoreductase confirmed its involvement in the reduction of the chromophoric group (N=N) of all the dyes.<sup>19</sup>

In other cases, the content of CYP450 and the specific activities of the superoxide dismutase were significantly increased compared to the control and surpass azoreductase activity after 4 h of decolorization. Plausible bioactive metabolites could have suppressed the activity of azoreductase and repressed the production of CYP450 and the activity of SOD.<sup>20–22</sup>

### Purification and characterization of azoreductase

The induced intracellular azoreductase for azo dye degradation was purified from *B. lentus* BI377 and precipitated with (NH<sub>4</sub>)<sub>2</sub>SO<sub>4</sub> (80%), followed by anion exchange column chromatography on DEAE-cellulose and size exclusion chromatography on Sephadex G-100 which allowed the recovery of 2.8 U in 2.6 mg ml<sup>-1</sup> of protein. The initial total amount of protein (34.8 mg ml<sup>-1</sup>), equivalent to an activity of about 0.41 U of azoreductase, was obtained from the crude extract of disrupted cells. The results of the purification of azoreductase from *B. lentus* BI377 are summarized in Table 2.

The effort has been successfully made to achieve 52.09 fold purification with 40% recovery (approximately) and 26.57 U mg<sup>-1</sup> of the total specific activity. The presence of a single band on both native and SDS-PAGE and a single band during

**Table 1** The whole cell activities during the decolourization of azo dyes<sup>a</sup>

Substrates	$\lambda_{\max}$ (nm)	Decolorization percentage		Azoreductase activity (U mg <sup>-1</sup> )			CYP450 content (nmol mg <sup>-1</sup> protein)			SOD (U mg <sup>-1</sup> )		
		4 h	6 h	0 h	4 h	6 h	0 h	4 h	6 h	0 h	4 h	6 h
<b>RR120</b>	530	75.2	97.7	0.051	0.071	0.074	0.031	0.032	0.062	422	492	762
<b>RR141</b>	540	85.4	98.9	0.044	0.062	0.065	0.031	0.041	0.066	431	484	766
<b>RR5</b>	550	76.7	95.8	0.046	0.074	0.078	0.037	0.040	0.058	437	474	858
<b>RR11</b>	550	79.6	97.7	0.048	0.068	0.071	0.025	0.031	0.054	425	461	854
<b>SY</b>	460	81.7	98.4	0.024	0.079	0.080	0.021	0.030	0.066	421	473	866
<b>Tartrazine</b>	470	85.7	97.2	0.033	0.084	0.088	0.024	0.029	0.071	424	489	871

<sup>a</sup> Note: All activities were recorded in triplicate and average values are mentioned in the table. Zeroth hour reading values are from control flasks.

**Table 2** Summary of the purification of azoreductase from *B. lentus* BI377

Purification step	Protein (mg ml <sup>-1</sup> )	Total activity (U)	Specific activity (U mg <sup>-1</sup> )	Purification fold
Crude extract	24.8	0.41	0.51	1.0
80% (NH <sub>4</sub> ) <sub>2</sub> SO <sub>4</sub>	3.16	1.26	12.05	23.62
Dialysis	2.82	1.52	16.22	31.8
Ion exchange	2.6	2.8	23.33	46.39
Gel filtration	0.6	2.65	26.57	52.09

gel filtration on a Sephadex G-100 column indicate the electrophoretic homogeneity (Fig. 1).

A specific activity of 26.57 U mg<sup>-1</sup> for azoreductase was noted after purification which corresponded to a 40% improvement as compared to the crude extract. Protein separation by SDS-PAGE resulted in a single band equivalent to a molecular mass of 32 kDa in agreement with previous

theoretical values of azoreductases from various bacterial isolates which have been used for azoic dye degradation.<sup>23a,b,24</sup>

#### Characterization and substrate specificity study of the purified azoreductase

To observe the effect of pH, the activity of the purified enzyme was monitored over a wide pH range (4–10). It was found that the enzyme azoreductase showed significant activity in the pH range of 7–9 as compared to other pH ranges, however, the optimum pH was established to be pH 8.0 (Fig. 2a).

These observations were quite similar to those for other azoreductases near to neutral pH.<sup>17,25,26</sup> Moreover, alkaliphilic strain *Bacillus lentus* always regulates its intracellular pH in such a way that it will remain near neutral.<sup>27</sup> Studies concerning the thermostability were performed at different temperature points of 40–100 °C at pH 8.0 (Fig. 2b). The azoreductase activity linearly increased in the temperature range from 40 to 70 °C but the optimum activity was found at 80 °C. The optimum pH and temperature conditions for purified enzyme were 8.0 and 80 °C respectively, nevertheless the maximum stability and maximum relative activity (≥70%) were observed in the range of 50 to 70 °C for three days. Very few scientific reports are available on thermostable alkaliphilic azoreductase at 80 °C, therefore this uniqueness could be beneficial for bioremediation even under extreme conditions.<sup>25</sup> To obtain the  $K_m$  and  $V_{max}$  value electron donor study, the enzyme activity was measured by varying the concentrations of one of the substrate dyes, NADH and NADPH, and keeping the concentration of another substrate fixed. Their individual values were determined by double reciprocal plots as shown in Table 3.

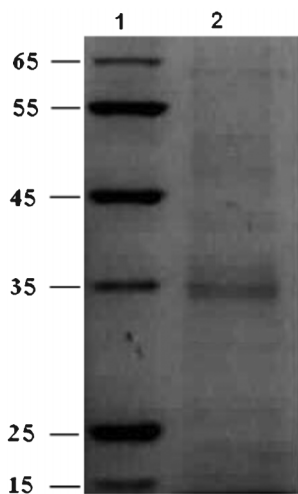


**Fig. 1** Molecular mass estimation of purified azoreductase by SDS-PAGE (lane 1: marker, lane 2: enzyme).

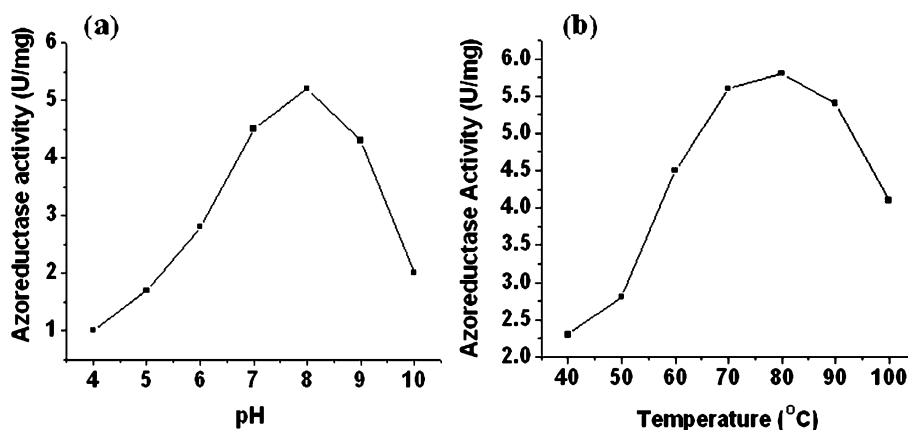


**Fig. 2** Effect of a) pH & b) temperature on purified azoreductase activity.

**Table 3** Kinetics parameters of purified azoreductase with TAR and electron donors<sup>a</sup>

Substrates	Azoreductase activity (U mg <sup>-1</sup> )	K <sub>m</sub> (μM)	V <sub>max</sub> (mmol min <sup>-1</sup> mg <sup>-1</sup> )	k <sub>cat</sub> (s <sup>-1</sup> )
Tartrazine	0.123 ± 0.007	0.20 ± 0.08	11 ± 2	4.5 ± 0.12
NADH	0.056 ± 0.005	0.32 ± 0.11	20 ± 5	4.6 ± 0.14
NADPH	0.042 ± 0.004	0.42 ± 0.04	13 ± 2	2.2 ± 0.13

<sup>a</sup> Note: All assays were done in triplicate. Values are mean ± standard deviation.

It was shown that the V<sub>max</sub> values are significantly close to each other, however, the catalytic efficiency of azoreductase in the presence of NADH was found to be higher than with NADPH. Hence, it was established that NADH dependant azoreductase is involved in the TAR reduction process.<sup>24</sup> The catalytic efficiency of the purified azoreductase was screened using azo dyes *viz.* RR120, RR141, RR5, RR11, SY and TAR which were used in whole cell decolorization previously. Eventually, study revealed that the purified enzyme azoreductase has a wide range of substrate specificity (ESI Table S1†). Nevertheless, it has shown maximum activity for TAR dye and minimum activity for RR11 dye. The highest activity against TAR as compared to other dyes may be due to the COONa group *ortho* and SO<sub>3</sub>Na group *para* to the azo bond. Both highly electronegative groups would withdraw the electrons from the azo bond *via* resonance, leading to the azo bond being more electrophilic and reductive for color removal.<sup>28</sup>

#### Identification of the purified azoreductase by MALDI-TOF

The protein band corresponding to the zone of clearing on the native PAGE assay was analyzed by trypsinolysis, MALDI-TOF mass spectrometry and database searching. Utilizing this approach, the principal protein in the band was identified as FMN containing NADH dependant azoreductase NCBI database information. After a database search, the purified protein was found to have a high sequence homology to FMN-dependent NADH-azoreductase of *Bacillus thuringiensis* (Accession No. ZP\_04075052.1) and *Bacillus cereus* AH1273 (Accession No. ZP\_04177368.1). The identification of the azoreductase was based on matching 9 of 16 experimental ion masses which were assigned from the most intense peaks (ESI Fig. S2†).

#### Spectrophotometric, bioanalytical, and enzyme analysis of azoaromatic degradation

UV-visible spectra analysis of the decolorized samples revealed that maximum decolorization was achieved within 8 h in the case of all substrate dyes. A significant decrease in the original absorbance maxima of the dye within two hours, and the appearance of new intense peaks at 450 nm after four hours indicated the formation of lower molecular weight aromatic metabolites.<sup>1,2,29</sup>

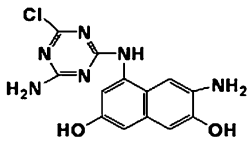
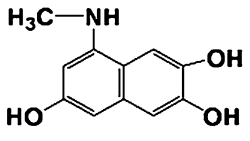
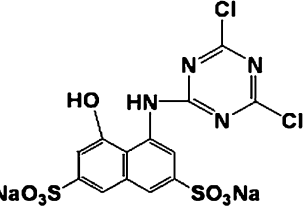
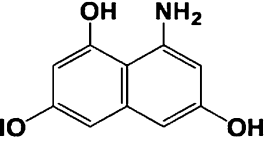
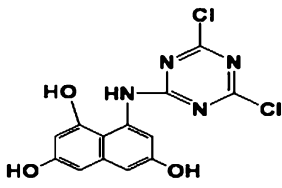
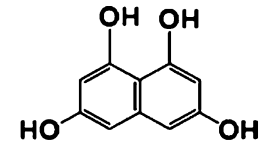
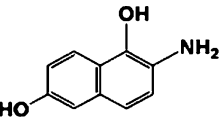
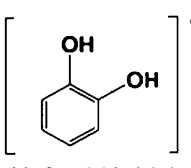
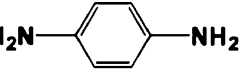
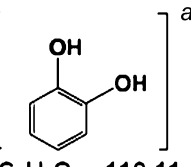
Based on the GC-MS (ESI Fig. S3†) and FTIR (ESI Fig. S4†) analysis of the intermediate metabolites, possible major fragmented products are illustrated in Table 4. In correlation to this, the formation of 5-(4-amino-6-chloro-1,3,5-triazinylamino)-3-aminonaphthalene-2,7-diol [318.72 *m/z*] (1), sodium 4-(4,6-dichloro-1,3,5-triazin-2-ylamino)-5-hydroxynaphthalene-2,7-disulfonate [511.22 *m/z*] (3), 8-(4,6-dichloro-1,3,5-triazin-2-

ylamino) naphthalene-1,3,6-triol [339.13 *m/z*] (5), 2-amino-naphthalene-1,6-diol [175 *m/z*] (7), and 1,4-diaminobenzene [108 *m/z*] (8) was established from GC-MS fragmentation (*m/z*) ions for the metabolites isolated after 4 h of incubation with RR141, RR11, RR5, SY and TAR respectively. Broad peaks were observed in the FTIR spectra at 4 h. Those at 3452.3 and 3500 cm<sup>-1</sup> were due to N-H stretching, those at 2921.0 to 2852.0 cm<sup>-1</sup> were due to C-H stretching and those at 1045.0 and 1032 cm<sup>-1</sup> were due to S-O stretching.<sup>30</sup> This helps to understand that the metabolites at 4 h *viz.*, 1, 3, 5, 7 and 9 are the cleaved products of azoreduction and simultaneous transformation.<sup>30-32</sup> Eventually, the enzyme activity study and spectroscopic data confirmed the involvement of azoreductase in the cleavage of the azo bond (N=N) thereby leading to the formation of aromatic amines under static conditions.<sup>30,33</sup> After 6 h, the major metabolites were found to be 8-(methylamino) naphthalene-2,3,6-triol [205.21 *m/z*] (2), 8-aminonaphthalene-1,3,6-triol [191.18 *m/z*] (4), naphthalene-1,3,6,8-tetraol [207.18 *m/z*] (6), as established by the GC-MS fragmentation *m/z* ion peaks and by FTIR frequencies at 2923, 2926, and 1660, cm<sup>-1</sup> for RR141, RR11 and RR5 respectively. After six hours, FTIR frequencies were observed at 2923, 2926, 2853 and 2850 cm<sup>-1</sup> for the C-H aliphatic stretch for RR141, RR11, SY and TAR metabolites respectively. A FTIR frequency at 3404 cm<sup>-1</sup> corresponding to the O-H stretch for metabolites of tartrazine confirmed the formation of lower molecular weight phenolic and/or aliphatic metabolites by an aerobic multistep conversion process. Metabolites 2, 4 and 6 were generated by the oxidation reaction.<sup>18,31,34,35</sup>

The CO binding spectra exhibited a characteristic induction in response to azo dyes and their intermediate metabolites (Fig. 3).

The magnitude of the peak at 450 nm increased just after the addition of RR120, RR141 and SY whereas those for RR5, RR11 and TAR appeared after 2 h of incubation till the process of mineralization was complete (8 h). Thus, the level of induction and content of CYP450 in the case of all dye degradations suggests its possible involvement in desulphonation as well as deamination of aromatic intermediate metabolites *via* hydroxylation.<sup>2,12,18</sup> The induction of SOD activity marked the generation of oxidative stress and indicated their subsequent action in the dismutation of reactive intermediate metabolites.<sup>9,21</sup> Hence, the entire process revealed the imperative redox potential of the strain *B. lentus* BI377 to carry out nonspecific azoaromatic mineralization by a mutually regulated process in the proximity of its outer membrane.<sup>13</sup> In due course, these biotransforming enzymes along with azoreductase were solely responsible for the degradation of the toxic dyes into aromatic amines and the

**Table 4** Summary of the major intermediate metabolites and % TOC during 4 to 6 h of decolorization/degradation<sup>a</sup>

Substrate dyes	Four hours of incubation Major intermediate metabolites	%TOC	Six hours of incubation Major intermediate metabolites	%TOC
RR141	 [1]C <sub>13</sub> H <sub>11</sub> ClN <sub>6</sub> O <sub>2</sub> , 318.72 (m/z)	11.3	 [2]C <sub>11</sub> H <sub>11</sub> NO <sub>3</sub> 205.21 (m/z)	2.24
RR11	 [3]C <sub>13</sub> H <sub>6</sub> Cl <sub>2</sub> N <sub>4</sub> Na <sub>2</sub> O <sub>7</sub> S <sub>2</sub> , 511.22 (m/z)	9.2	 [4]C <sub>10</sub> H <sub>9</sub> NO <sub>3</sub> 191.18 (m/z)	1.29
RR5	 [5]C <sub>13</sub> H <sub>8</sub> Cl <sub>2</sub> N <sub>4</sub> O <sub>3</sub> 339.13 (m/z)	9.7	 [6]C <sub>10</sub> H <sub>9</sub> NO <sub>4</sub> 207.18 (m/z)	1.58
SY	 [7]C <sub>10</sub> H <sub>9</sub> NO <sub>2</sub> 175.18 (m/z)	8.2	 [8]C <sub>6</sub> H <sub>6</sub> O <sub>2</sub> 110.11 (m/z)	0.42
TAR	 [9]C <sub>6</sub> H <sub>8</sub> N <sub>2</sub> 108.14 (m/z)	7.9	 [10]C <sub>6</sub> H <sub>6</sub> O <sub>2</sub> 110.11 (m/z)	0.51

<sup>a</sup> Note: The metabolites **8** and **10** were not detected due to an insufficient quantity of sample for characterization. They are proposed plausible intermediates during the degradation process of SY and TAR respectively.

further opening of all aromatic nuclei to aliphatic form and their subsequent transformation to CO<sub>2</sub> and H<sub>2</sub>O under microaerophilic conditions.<sup>12,13,18</sup> HPLC analysis of the degradation product of TAR showed major peaks at retention times of 3.15 and 3.69 min.

After comparing these intermediate metabolites with standards it was found that the peak of 1,4-diaminobenzene (retention time 3.18 min) corresponds to the chromatogram of

the 4 h intermediate metabolites of TAR degradation (Fig. 4), which supported the strong possibility of the formation of 1,4-diaminobenzene by the reduction mechanism of azoreductase by cleaving the azo linkage (N=N) which was further confirmed by GC-MS and FTIR and enzymatic studies (as discussed earlier). Hence, under this notion, the proposed pathway of tartrazine reduction could be illustrated as shown in Fig. 5.

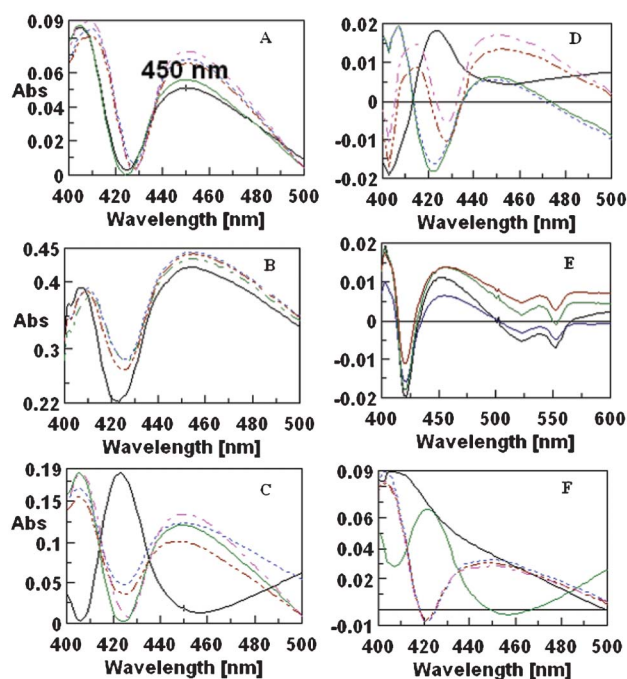


**Fig. 3** The CO-binding cytochrome P450 spectra of A) RR120, B) RR141, C) RR5, D) RR11, E) SY and F) TAR decolorization/degradation [— (0 h), --- (2 h), - - - (4 h), - - - (6 h), - - - (8 h)].

Analysis could not succeed in isolating the intermediate catechol during each dye degradation but the resemblance of most the metabolites (7 and 9 in Table 4) strongly suggested its existence (8 and 9)<sup>18,35,36</sup> and its further utilization by the central metabolic pathway.<sup>36,37</sup> The progress of catechol metabolism by *B. lentus* BI377 was monitored by measuring

quinone related metabolites resulting from the tyrosinase enzyme activity (data not shown). The activity of tyrosinase remains unchanged during dye degradation, suggesting the possible oxidative cleavage of catechol into aliphatic metabolites *via* the *cis*-muconic acid pathway.<sup>18,38</sup> Eventually, the trace of aliphatic metabolites and decreasing % TOC (Table 4) confirmed that the recalcitrant sulphonated dyes' degradation pathway leads to complete mineralization *via* the TCA cycle.<sup>2,30</sup>

## Experimental

### Chemicals

DEAE-cellulose and Sephadex G-100 were purchased from Sigma Aldrich, USA. Precision plus Protein Standard 161-0373EDU was purchased from Bio-Rad, USA and NADH was procured from SRL Chemicals, India. All azo dyes *viz.* RR120, RR141, RR2, RR11, SY and TAR were procured from a textile plant in Solapur, India (see the molecular structure in ESI Fig. S 5†). All other chemicals were of the highest grade of purity.

### Microorganism, growth medium and culture condition

The soil isolate *B. lentus* BI377 was grown in nutrient broth (NB) containing ( $\text{g l}^{-1}$ ) peptone, 5; yeast extract, 5; and NaCl, 5, aerobically at 40 °C for 24 h in Erlenmeyer flasks (500 ml capacity).<sup>18</sup> The media pH 8.0 was adjusted by sodium phosphate buffer using a EUTECH-510 pH meter.<sup>18</sup>

### Decolourization assessment with whole cell activity

To study the whole cell activity during decolorization, the strain was grown in 100 ml of the same medium in 500 ml Erlenmeyer flasks for 12 h at 40 °C under static conditions before the addition of substrate azo dyes to a final concentration of 10  $\text{mg l}^{-1}$ . A control sample measurement was done

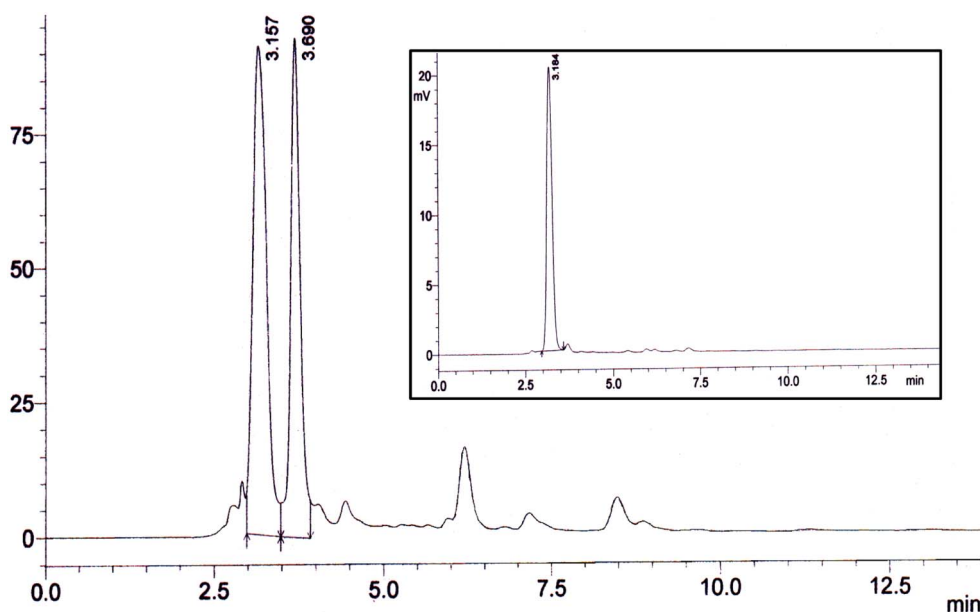


**Fig. 4** HPLC chromatogram of TAR degradation at 4 h and 1,4-diaminobenzene standard (inset).

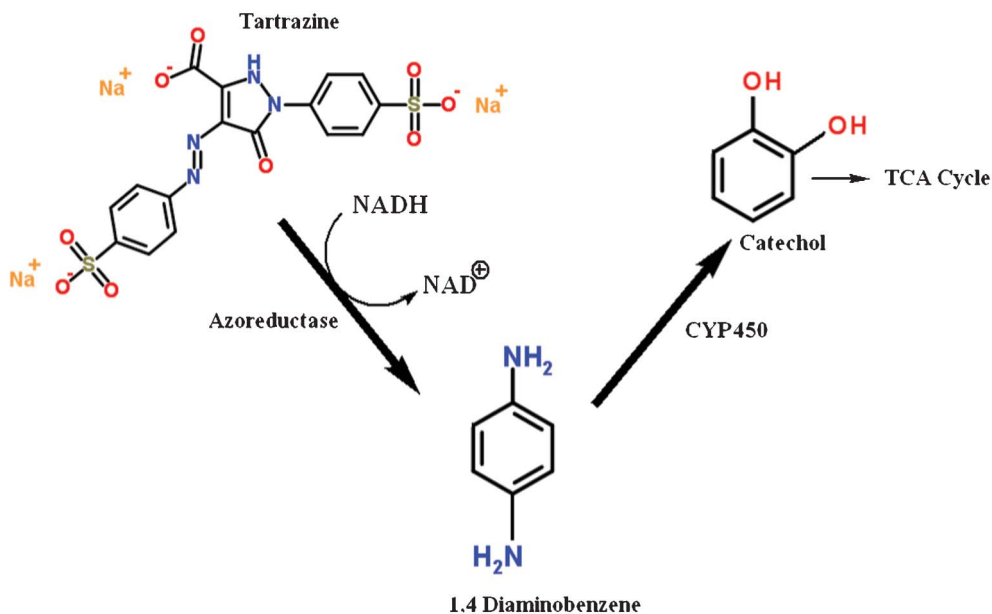


Fig. 5 Proposed pathway of TAR degradation by *B. lentus* BI377.

before the addition of the dye at 0 h. Decolorised sample aliquots were withdrawn from the control and the decolorised sample flask at 2 h intervals and centrifuged at 10 000g for 15 min using a DuPont Sorvall RC-5B refrigerated centrifuge and the same procedure was repeated till the maximum decolorization was obtained. The supernatant was used to determine the percentage of decolorization by spectrophotometric measurement<sup>19</sup> and the pelleted cell mass was suspended in 50 mM sodium phosphate buffer (pH 7.2) for enzyme study.

#### Preparation of the cell free extract and enzyme assays

The pelleted cell mass was resuspended in the same buffer and centrifuged three times to remove the residue of the dyes. Cell disruption was carried out by using a probe sonicator (6 s cycle and 60 Hz by Sonoplus HD 70, Bandelin, Berlin, Germany). The resulting homogenate was centrifuged at 10 000g for 30 min at 4 °C and the supernatant was used for enzyme purification. The protein concentration was estimated by Lowry's method.<sup>40</sup> The azoreductase activity was determined according to the protocol of Zimmermann<sup>23b</sup> with slight modification. In a typical procedure, the reaction mixture containing 100 mM phosphate buffer (pH 7.4), 2 mM NADH, 150 μM of carmosine dye and 100 μl of the enzyme was pre-incubated for 10 min. The reaction was then initiated by addition of (1 mM) NADH and monitored for the decrease in absorbance at 515 nm. One unit (U) of enzyme activity was defined as the amount of the enzyme required to reduce 1 μmol of substrate dye per minute per milligram of protein. CYP450 content was estimated using the method of Omura and Sato, 1964.<sup>41</sup> Superoxide dismutase activity was measured spectrophotometrically according to Mishra and Fridovich<sup>42</sup> on a spectrophotometer at 37 °C. The autooxidation of epinephrine (formation of adrenochrome) was measured at 480 nm at the interval of 40 s for 5 min.

#### Purification of the azoreductase enzyme

The crude cell free extract was subjected to ammonium sulphate precipitation. In the resulting supernatant the addition of ammonium sulphate was continued to get 80% saturation. The precipitated protein was separated by centrifugation in cold conditions and was dissolved in phosphate buffer pH 7.0 (0.1 M). The activity of azoreductase and the protein concentration was determined at the end of each purification step. Redissolved precipitate was dialyzed against the same buffer and was stored at 4 °C for further purification. After the dialysis, the sample was applied to a DEAE-cellulose column (2 cm × 45 cm) equilibrated and washed with 0.1 M phosphate buffer (pH 7.0) and eluted enzyme. The enzyme was eluted from the DEAE-cellulose column by phosphate buffer pH 7.0 (0.1 M) containing 0 to 0.5 M NaCl linear gradient at a flow rate 4 ml for 15 min. The fractions with the maximum activity of azoreductase were pooled together and loaded on a Sephadex G-100 column. The protein was eluted by phosphate buffer and the fraction of 4 ml each was collected at the rate of 1 ml min<sup>-1</sup>. The fractions with the maximum activity were pooled together and concentrated by reverse dialysis. The purity of the enzyme was judged by polyacrylamide gel electrophoresis according to Laemmli 1970 with slight modification.<sup>43</sup> The molecular weight of the enzyme was determined by comparing the electrophoretic mobility of the enzyme with Precision plus Protein Standards (Bio-Rad USA, Precision plus Protein All Blue Standards 161-0373EDU).

#### Characterization study of a purified azoreductase

The effect of pH on azoreductase activity was determined by incubating the reaction mixture at pH values ranging from 4 to 10 using the standard buffer systems of acetate buffer for pH 4 to 6, phosphate buffer for 6 to 7 and tris buffer for 8 to 10.0. Stability was determined by measuring the residual activity of

the enzyme after 30 min of pre incubation in buffers of various pH values from 4 to 9 at 35 °C. The optimum temperature for enzyme activity was determined by conducting the assay at various temperatures of 25, 30, 35, 40, 45 and 50 °C in 100 mM phosphate buffer at pH 7.0. The residual activity was determined as per the standard assay procedure for the azo reductase activity. A substrate specificity study was performed by studying the reduction of six azo dyes *viz.*, RR120, RR141, RR2, RR11, SY and TAR as substrates with purified azoreductase from the strain *B. lentus* BI377. The electron donor study was also performed using 0.5–5.0 mM solution concentration of NADH and NADPH for 30 min at 35 °C. The values of Michaelis–Menten constant ( $K_m$ ) and maximal velocity ( $V_{max}$ ) for the enzyme with TAR was obtained by Lineweaver–Burk double reciprocal plots.

#### Protein identification by matrix assisted laser desorption/ionization time of flight (MALDI-TOF)

MALDI MS/MS analysis was performed on a SYNAPT HDMS system (Waters Corporation, Milford, USA). Protein sample digests were reconstituted in 5% ACN containing 0.1% TFA and premixed with an equal volume of 10%  $\alpha$ -cyano-4-hydroxycinnamic acid (CHCA) matrix and applied on to a 96 well MALDI plate. All samples were acquired on a 200 Hz solid state UV laser in V mode by MassLynx 4.1. The quadrupole profile was set to 500  $m/z$  for 5% of the scan time and then ramped to 1500  $m/z$  for remaining period of the scan. The instrument mass calibration was carried with polyethylene glycol (PEG). Proteins were identified by the MALDI survey method, involving a combination of PMF and tandem mass spectrometric (MS/MS) approaches for the identification of proteins. In the MS survey method spectra were recorded in the mass range of 800 to 4000  $m/z$  for 60 s. MS/MS analysis was performed in a data dependent manner for the top 7 peptides with higher relative intensity for 30 s each and the product ion mass range was set to 100 to 1500  $m/z$ . For protein identification MS/MS data were processed by PLGS software, searched against the UniProt Bacillus database with the mass tolerance set to 100 ppm, carbamidomethylation as the fixed modification and methionine oxidation as the variable modification.<sup>26</sup>

#### UV-visible, GC-MS, FTIR and HPLC study of the intermediate metabolites

The culture media was modified with 50 mg of each substrate dye for the spectroscopic observations of decolorization study in 500 ml capacity Erlenmeyer flasks with a control flask (without dye). Decolorized samples were collected from each at two hour intervals till the maximum decolourisation was observed. Absorption of the supernatant was monitored at the appropriate wavelength for each dye. Percentage decolourisation was calculated using the difference between initial and final optical density. Metabolites were extracted from the supernatants using methanol, ethyl acetate or dichloromethane (DCM) and after rotaevaporation were dried over anhydrous sodium sulfate.<sup>44</sup> The extracted metabolites were subjected to thin layer chromatography (TLC) using 15% methanol : 15% ammonium hydroxide/acetonitrile as the mobile phase. 25  $\mu$ l of the sample was subjected to HPLC

analysis using a C-18 reverse phase column with a solvent system consisting of methanol and water (v/v). A linear gradient from 20% methanol (isocratic for the initial 2 min) increased to 100% over 10 min and then maintained at 100% concentration for 10 min with a flow rate at 1 ml min<sup>-1</sup>.<sup>34</sup> The degradation products were monitored at 230 nm. Fourier Transform Infrared spectroscopy (FTIR) studies of the metabolites were carried out using the KBr pellet technique in the wavenumber range of 400–4000 cm<sup>-1</sup> on a Shimadzu-8400 FTIR spectrophotometer. Gas chromatography–mass spectroscopy (GC-MS) analysis was performed using a GB5 column with a 15–20 min runtime on a Shimadzu-GC-MS-QP5050. TOC analysis was performed as described by the dichromate method of Walkely and Black<sup>45</sup> and % removal was calculated using the protocol of Saratale *et al.*<sup>39</sup>

## Conclusion

The present study emphasizes the major utility of isolate *B. lentus* BI377 for the bioremediation of hazardous recalcitrant azoaromatic compounds. The astonishing catabolic ability of the strain certainly provides unparalleled opportunities for understanding the fundamental molecular mechanism of the degradation of organic compounds and their utilization as an energy source. The purified and characterized flavin containing alkaliphilic azoreductase provides rich opportunities to investigate the nonspecific diverse substrate specificity and mechanism of promiscuity among the family of flavoproteins. This study opens up a dependable and efficient way to use *B. lentus* to accelerate the exploration of the feasibility of the bioremediation reactions over a wide range of temperature and pH. The symbiotic action of the enzyme azoreductase, cytochrome P450 monooxygenase and superoxide dismutase may provide a selective advantage to the degradation reaction under various conditions of environmental stress. Therefore, this bacterial strain provides the potential enzymatic machinery to remove a wide variety of natural and man-made aromatic compounds discharged through geochemical cycles and urban and industrial activities as well as their subsequent transformation into CO<sub>2</sub> and H<sub>2</sub>O.

## Acknowledgements

Author Chetan C. Oturkar gratefully acknowledges the University Grants Commission (UGC, New Delhi), Government of India for research and Dr Kothari's postdoctoral fellowship.

## References

- 1 A. Stolz, *Appl. Microbiol. Biotechnol.*, 2001, **56**, 69–80.
- 2 A. Pandey, P. Singh and L. Iyengar, *Int. Biodeterior. Biodegrad.*, 2007, **59**, 73–84.
- 3 G. Mishra and M. Tripathy, *Colourage*, 1993, **40**, 35–40.

- 4 S. Mendes, A. Farinha, C. G. Ramos, J. H. Leitao, C. A. Viegas and L. O. Martins, *Bioresour. Technol.*, 2011, **102**, 9852–9859.
- 5 A. Khalid, M. Arshad and D. E. Crowley, *Appl. Microbiol. Biotechnol.*, 2008, **78**, 361–369.
- 6 C. I. Pearce, R. Christie and C. Boothman, *Biotechnol. Bioeng.*, 2006, **95**, 692–703.
- 7 A. Ryan, N. Laurieri, I. Westwood, C. J. Wang, E. Lowe and E. Sim, *J. Mol. Biol.*, 2010, **400**, 24–37.
- 8 E. Cabiscol, J. Tamarit and J. Ros, *Int. Microbiol.*, 2000, **3**, 3–8.
- 9 H. Ben Mansour, D. Corroler, D. Barillier, K. Ghedira, L. Chekir and R. Mosrati, *Food Chem. Toxicol.*, 2007, **45**, 1670–1677.
- 10 P. A. Williams, J. Cosme, V. Sridhar, E. F. Johnson and D. E. McRee, *J. Inorg. Biochem.*, 2000, **81**, 183–90.
- 11 Ju. Kou-San and P. E. Rebecca, *Microbiol. Mol. Biol. Rev.*, 2010, **74**(2), 250–272.
- 12 O. Sterner, *Chemistry, Health and Environment*. Wiley-VCH, 1999. Weinheim, Germany.
- 13 M. Xu, J. Guo and G. Sun, *Appl. Microbiol. Biotechnol.*, 2007, **76**, 719–726.
- 14 L. Pereira, A. Coelho, A. C. Viegas, C. Ganachaud, G. Lacazio, T. Tron, M. Robalo and L. O. Martins, *Adv. Synth. Catal.*, 2009, **351**, 1857–1865.
- 15 T. Imagawa, T. Tsurumura, Y. Sugimoto, K. Aki, K. Ishidoh, S. Kuramitsu and H. Tsuge, *J. Biol. Chem.*, 2011, **286**, 44078–85.
- 16 A. Erkurt, *Biodegradation of Azo Dyes-The Handbook of Environmental Chemistry*, Springer, Heidelberg, Dordrecht, London, New York, 2010.
- 17 K. Matsumoto, Y. Mukai, D. Ogata, F. Shozui, J. N. Nduko, S. Taguchi and T. Ooi, *Appl. Microbiol. Biotechnol.*, 2010, **86**(5), 1431–8.
- 18 C. Oturkar, H. Nemade, P. Mulik, M. Patole, R. Hawaldar and K. Gawai, *Bioresour. Technol.*, 2011, **102**, 758–764.
- 19 B. Y. Chen, *Process Biochem.*, 2002, **38**(3), 437–446.
- 20 H. Xu, T. M. Heinze, S. Chen, C. E. Cerniglia and H. Chen, *Appl. Environ. Microbiol.*, 2007, **73**(23), 7759–7762.
- 21 M. T. Madigan, J. M. Martinko and J. Parker, *Brock Biology of Microorganisms*, 10th edn, Prentice-Hall, Upper Saddle River, 2003.
- 22 P. Tang, J. K. Liu, S. M. Chou, L. I. Hor, W. J. Chen and S. C. Chen, *Process Biochem.*, 2008, **43**, 753–757.
- 23 (a) T. Zimmermann, F. Gasser, H. G. Kulla and T. Leisinger, *Arch. Microbiol.*, 1984, **138**(1), 37–43; (b) T. Zimmermann, H. G. Kulla and T. Leisinger, *Eur. J. Biochem.*, 1982, **129**(1s), 197–203.
- 24 S. Punj and H. Gilbert, *Curr. Issues Mol. Biol.*, 2008, **11**, 59–66.
- 25 J. Maier, A. Kandelbauer, A. Erlacher, A. Cavaco-Paulo and G. M. Gubitz, *Appl. Environ. Microbiol.*, 2004, **70**(2), 837–844.
- 26 D. Cui, D. Li, X. Zhao, C. Gu, L. Wang and M. Zhao, *Process Biochem.*, 2012, **47**, 544–549.
- 27 C. R. Aono, M. Ito and K. Horikoshi, *Microbiology*, 1997, **143**, 2531–2536.
- 28 C. C. Hsueh, B. Y. Chen and C. Y. Yen, *J. Hazard. Mater.*, 2009, **167**, 995–1001.
- 29 M. Isik and D. T. Sponza, *Process Biochem.*, 2003, **38**, 1183–1192.
- 30 R. V. Khandare, N. R. Rane, T. R. Waghmode and S. P. Govindwar, *Environ. Sci. Pollut. Res.*, 2012, **19**, 1709–1718.
- 31 F. Gosetti, V. Gianotti, S. Polati and M. C. Gennaro, *J. Chromatogr., A*, 2005, **1090**, 107–115.
- 32 S. S. Phugare, D. C. Kalyani, A. V. Patil and J. P. Jadhav, *J. Hazard. Mater.*, 2011, **186**, 713–723.
- 33 H. Chen, *Curr. Protein Pept. Sci.*, 2006, **7**, 101–111.
- 34 S. Kalme, G. Ghodake and S. Govindwar, *Int. Biodeterior. Biodegrad.*, 2007, **60**, 327–333.
- 35 C. V. Nachiyar and G. S. Rajkumar, *Chemosphere*, 2004, **57**, 165–169.
- 36 J. S. Chang, C. Chou and S. Y. Chen, *Process Biochem.*, 2001, **36**, 757–763.
- 37 M. Ferraroni, I. P. Solyanikova, M. P. Kolomytseva, A. Scozzafava, L. Golovleva and F. Briganti, *J. Biol. Chem.*, 2004, **279**(26), 27646–27655.
- 38 M. R. G. Pereira, E. S. de Oliveira, F. A. G. A. de Villar, M. S. Grangeiro, J. Fonseca, A. R. Silva, M. F. D. Costa, S. L. Costa and R. S. El-Bachá, *J. Bras. Patol. Med. Lab.*, 2004, **40**, 280–285.
- 39 R. G. Saratale, G. D. Saratale, J. S. Chang and S. P. Govindwar, *Biodegradation*, 2010, **21**(6), 999–1015.
- 40 O. H. Lowry, N. J. Rousebrough, A. L. Farr and R. J. Randall, *J. Biol. Chem.*, 1951, 265–275.
- 41 T. Omura and R. Sato, *J. Biol. Chem.*, 1964, **239**, 2379–2385.
- 42 H. P. Misra and I. Fridovich, *J. Biol. Chem.*, 1972, **247**(10), 3170–3175.
- 43 U. K. Laemmli, *Nature*, 1970, **227**, 680–5.
- 44 I. Soojhawon, P. D. Lokhande, K. M. Kodam and K. R. Gawai, *Enzyme Microb. Technol.*, 2005, **37**, 527–533.
- 45 A. Walkely and A. I. Black, *Soil Sci.*, 1934, **37**, 29–38.